AFRL-ML-WP-TP-2007-527

EFFECTS OF SOLVATION ON ONE- AND TWO-PHOTON SPECTRA OF COUMARIN DERIVATIVES: A TDDFT STUDY (PREPRINT)

Kiet A. Nguyen, Paul N. Day, and Ruth Pachter

Hardened Materials Branch
Survivability and Sensor Materials Division

OCTOBER 2006

AIR FORCE RESEARCH LABORATORY
MATERIALS AND MANUFACTURING DIRECTORATE
WRIGHT-PATTERSON AIR FORCE BASE, OH 45433-7750
AIR FORCE MATERIEL COMMAND
UNITED STATES AIR FORCE

NOTICE AND SIGNATURE PAGE

Using Government drawings, specifications, or other data included in this document for any purpose other than Government procurement does not in any way obligate the U.S. Government. The fact that the Government formulated or supplied the drawings, specifications, or other data does not license the holder or any other person or corporation; or convey any rights or permission to manufacture, use, or sell any patented invention that may relate to them.

This report was cleared for public release by the Air Force Research Laboratory Wright Site (AFRL/WS) Public Affairs Office and is available to the general public, including foreign nationals. Copies may be obtained from the Defense Technical Information Center (DTIC) (http://www.dtic.mil).

AFRL-ML-WP-TP-2007-527 HAS BEEN REVIEWED AND IS APPROVED FOR PUBLICATION IN ACCORDANCE WITH ASSIGNED DISTRIBUTION STATEMENT.

*//Signature//

RUTH PACHTER, Ph.D.
Computational Materials Project
Exploratory Development
Hardened Materials Branch

//Signature//

MARK S. FORTE, Acting Chief
Hardened Materials Branch
Survivability and Sensor Materials Division

//Signature//

TIM J. SCHUMACHER, Chief
Survivability and Sensor Materials Division

This report is published in the interest of scientific and technical information exchange, and its publication does not constitute the Government's approval or disapproval of its ideas or findings.

*Disseminated copies will show "//Signature//" stamped or typed above the signature blocks.

REPORT DOCUMENTATION PAGE

Form Approved
OMB No. 0704-0188

1. REPORT DATE *(DD-MM-YY)*	2. REPORT TYPE	3. DATES COVERED *(From - To)*
October 2006	Journal Article Preprint	

4. TITLE AND SUBTITLE

EFFECTS OF SOLVATION ON ONE- AND TWO-PHOTON SPECTRA OF COUMARIN DERIVATIVES: A TDDFT STUDY (PREPRINT)

5a. CONTRACT NUMBER
In-house

5b. GRANT NUMBER

5c. PROGRAM ELEMENT NUMBER
62102F

6. AUTHOR(S)

Kiet A. Nguyen (UES, Inc.)
Paul N. Day (General Dynamics Information Technology, Inc., formerly Anteon Corporation)
Ruth Pachter (AFRL/MLPJE)

5d. PROJECT NUMBER
4348

5e. TASK NUMBER
RG

5f. WORK UNIT NUMBER
M08R1000

7. PERFORMING ORGANIZATION NAME(S) AND ADDRESS(ES)

UES, Inc.
Dayton, OH 45432

General Dynamics Information Technology, Inc.
5100 Springfield Pike, Suite 509
Dayton, OH 45431-1264

Hardened Materials Branch (AFRL/MLPJE)
Survivability and Sensor Materials Division
Materials and Manufacturing Directorate
Wright-Patterson Air Force Base, OH 45433-7750
Air Force Materiel Command
United States Air Force

8. PERFORMING ORGANIZATION REPORT NUMBER
AFRL-ML-WP-TP-2007-527

9. SPONSORING/MONITORING AGENCY NAME(S) AND ADDRESS(ES)

Air Force Research Laboratory
Materials and Manufacturing Directorate
Wright-Patterson Air Force Base, OH 45433-7750
Air Force Materiel Command
United States Air Force

10. SPONSORING/MONITORING AGENCY ACRONYM(S)
AFRL/MLPJE

11. SPONSORING/MONITORING AGENCY REPORT NUMBER(S)
AFRL-ML-WP-TP-2007-527

12. DISTRIBUTION/AVAILABILITY STATEMENT
Approved for public release; distribution unlimited.

13. SUPPLEMENTARY NOTES

Journal article submitted to the Journal of Chemical Physics.

The U.S. Government is joint author of this work and has the right to use, modify, reproduce, release, perform, display, or disclose the work.

PAO Case Number: AFRL/WS 06-2297, 27 Sep 2006.

14. ABSTRACT

We report one- (OPA) and two-photon absorption (TPA) excitation energies and cross sections for a series of 7-aminocoumarins using time-dependent density functional theory with various basis sets and functionals, including exchange-correlation functionals using the Coulomb-attenuating method (CAMB3LYP and mCAMB3LYP), to evaluate their performance in gas-phase and in solvents. Except for the CAMB3LYP results , the computed OPA excitation energies and transition dipole moments are in good agreement with experiment. The range of errors obtained from various functionals is discussed in detail. The relationship of donor and acceptor groups with OPA and TPA resonances and intensities is also discussed.

15. SUBJECT TERMS

One-photon absorption (OPA), two-photon absorption (TPA), Coulomb-attenuating method, (CAMB3LYP and mCAMB3LYP)

16. SECURITY CLASSIFICATION OF:			17. LIMITATION OF ABSTRACT:	18. NUMBER OF PAGES	19a. NAME OF RESPONSIBLE PERSON (Monitor)
a. REPORT	b. ABSTRACT	c. THIS PAGE			Ruth Pachter
Unclassified	Unclassified	Unclassified	SAR	40	19b. TELEPHONE NUMBER *(Include Area Code)* N/A

Standard Form 298 (Rev. 8-98)
Prescribed by ANSI Std. Z39-18

Effects of solvation on one- and two-photon spectra of coumarin derivatives: A TDDFT study

Kiet A. Nguyen,[a,b]* Paul N. Day,[a,c] and Ruth Pachter[a,]*

Materials and Manufacturing Directorate, Air Force Research Laboratory,

Wright-Patterson Air Force Base, OH 45433.

*Corresponding author

[a]Air Force Research Laboratory

[b]UES, Inc.

[c]Anteon Corporation.

ABSTRACT

We report one- (OPA) and two-photon absorption (TPA) excitation energies and cross sections for a series of 7-aminocoumarins using time-dependent density functional theory with various basis sets and functionals, including exchange-correlation functionals using the Coulomb-attenuating method (CAMB3LYP and *m*CAMB3LYP), to evaluate their performance in the gas-phase and in solvents. Except for the CAMB3LYP results, the computed OPA excitation energies and transition dipole moments are in good agreement with experiment. The range of errors obtained from various functionals is discussed in detail. The relationship of donor and acceptor groups with the OPA and TPA resonances and intensities is also discussed.

Keywords:

Two-photon

Cross-section

Excitation energies

Excited-state

Coumarin 120, 1, 480, 152, 152A, 522, 153, 307, 151.

1. Introduction

Coumarin derivatives that are formed by various substitutions of amino groups at the 7-position are widely used as probes in ultrafast solvation studies, as laser dyes,[1,2] and as nonlinear optical chromophores[3-5] in optoelectronic devices. Thus, pertinent optical properties for these applications have been extensively reported in the literature. Electronic one-photon absorption (OPA) spectra of coumarins, in particular, have been characterized in high temperature vapors,[6,7] in a supersonic jet expansion,[6-8] and in a variety of polar and nonpolar solvents.[9-15] Experimental studies have revealed the polar nature of the first excited state, which has been characterized as an intramolcular charge-transfer (ICT) state with a larger dipole moment than in the ground state. The large difference in dipole moment between the ground and excited states ($\Delta\mu_{ge}$) provides a viable mechanism for the intense two-photon absorption (TPA)[16-19] and other nonlinear processes[3,4] that have been observed and quantified for a number of coumarin derivatives.

Theoretically, OPA properties of coumarins in the gas-phase have been reported in semiemperical studies using AM1[20], PM3[21,22] and MNDO[23] methods. Recently, Cave et al.[24] reported a detailed theoretical study of coumarin 120 (C120) and C151 using a wide range of electronic structure methods to evaluate various ground and excited state properties. They found that using time-dependent density functional theory (TDDFT)[25-28] with hybrid functionals gives excellent agreement with S_0-S_1 experimental OPA excitation energies. In another survey[29] involving C102, C152, C153, and C343, excellent agreement with experiments was also reported for TDDFT excitation energies. Optical properties of C120,[24] C151,[24,30-32] 152A (C35, C481)[30,31] and C153[30,31] have been studied using TDDFT with continuum,[24] and explicit[30-32] solvent models. More recently, Ingrosso et al. reported[33] a solvation study of C153 in supercritical fluoroform using TDDFT with Becke's three-parameter (B3LYP)[34-36] hybrid functional. The successful applications of TDDFT with hybrid functionals for coumarins are consistent with our previous studies[37] on the prediction of excitation energies involving charge-transfer

excited states. However, we found the B3LYP functional[34-36] and the hybrid functional of Perdew, Burke, and Erzerhof (PBE0)[38,39] underestimate the experimental excitation energies of a number of ICT chromophores. Both functionals were found to overestimate the oscillator strengths for the first ICT excited-states. The failures to provide a good description for ICT excited states have been attributed to the incorrect long-range behavior of the exchange potential.[40,41] Thus, a detailed comparison between computed and experimental OPA and TPA excitation energies and intensities for a series of coumarins were carried out to assess the accuracy that can be achieved with the B3LYP, PBE0, and the new long-range-corrected (LC) functional of Janai et al.[40,41] Previous TDDFT studies on coumarins focused on the OPA excitation energy but not on intensity, and TPA spectra were not considered.

The aim of the present work is to investigate both the OPA and TPA spectra for a series of coumarin derivatives with different degrees of ICT characters (Figures 1 and 2) in the gas-phase and in solvents. In 7-aminocoumarins, the amine and carbonyl moieties are expected to act as electron donor and acceptor, respectively. Thus, the 4-methyl coumarin derivatives (Figure 1) with increasing degree of alkylation measure the effects of different donor groups on the OPA and TPA spectra. Effects of the acceptor are also gauged by 4-trifluoromethyl coumarin derivatives (Figure 2).

2.Computational Methods

The computation of excitation energies and cross sections was preceded by the determination of equilibrium geometries, and then single point excited state calculations were carried out to obtain the vertical excitation energies, transition dipoles, and oscillator strengths. All structures have been predicted using the Kohn-Sham (KS)[42] density functional theory with the 6-311G(d,p)[43] basis set and the B3LYP hybrid functional.[34-36] These structures were verified to be minima on the potential energy surface with harmonic frequency calculations using the Gaussian 03 program.[44] TDDFT calculations were carried out using the 6-311G(d,p), 6-311++G(d,p), and aug-cc-pVTZ (for selected cases) basis sets with the B3LYP, PBE0, and the new hybrid functional of Yanai et al.,[40] as implemented in the Dalton program.[45] This hybrid functional, called CAMB3LYP, combines properties of B3LYP and the long-range-correction for the exchange potential by an Ewald split of the r_{12}^{-1} operator into[40]

$$r_{12}^{-1} = \frac{1-\left[\alpha+\beta\cdot\mathrm{erf}(\mu r_{12})\right]}{r_{12}} + \frac{\alpha+\beta\cdot\mathrm{erf}(\mu r_{12})}{r_{12}}, \quad (1)$$

where μ, α, β are empirical parameters. Yanai et al. found that the CAMB3LYP functional yields the smallest error (MAE = 2.53 kcal/mol) with μ = 0.33, α = 0.19, and β = 0.46 ($\alpha + \beta$ = 0.65) in atomization energies for the G2 set. This is slightly better than the corresponding MAE of 2.68 kcal/mol for B3LYP, which is nearly equivalent to setting α = 0.2 and β = 0.0 in CAMB3LYP.[41] However, the ICT excitation energies for a model dipeptide are greatly improved, when compared to the CASPT2 results. In addition, we tested a modified CAMB3LYP (*m*CAMB3LYP) functional with a two-parameter Ewald split of the r_{12}^{-1} operator as,

$$r_{12}^{-1} = \frac{1-\left[\alpha+\alpha\cdot\mathrm{erf}(\mu r_{12})\right]}{r_{12}} + \frac{\alpha+\alpha\cdot\mathrm{erf}(\mu r_{12})}{r_{12}}, \quad (2)$$

where μ and α are kept unchanged.

To account for the solvent effects, TDDFT calculations were carried out with the nonequilibrium polarizable continuum model[46,47] (PCM) and the self-consistent reaction field (SCRF) model of Mikkelsen et al.,[48] which uses a spherical solute cavity (SCRF-S). The PCM solute cavities were carried out using the united atom topological model and empirical solvent radii, as implemented in the Gaussian 03 program.[44] The radii (a_0) for the SCRF-S were obtained using the largest interatomic distances of the solutes with added adjustments for van der Waals interactions. The SCRF-S calculations were carried out using the Dalton program.[45]

The TPA cross sections can be obtained by relating the absorption rate[37,49] to the TPA transition probability, which was first derived by Goppert-Mayer using second order perturbation theory.[50] The two photon absorptivity δ_{f0} between the ground-state (0) and the final state *f* is written as[37,51,52]

$$\delta_{f0}(E_1,E_2) = \frac{8\pi^4}{(ch)^2} E_1 E_2 \sum_f g_{f0}(E_1,E_2)\left|S_{f0}(E_1,E_2)\right|^2, \quad (3)$$

where c is the speed of light, h is the Planck's constant, E_λ the photon energies, $g_{f0}(E_1,E_2)$ is the normalized line shape function for the ground to *f* transition, which can be represented by a Gaussian or a Lorentzian. The two-photon matrix elements $S_{f0}(E_1,E_2)$ were obtained from single- (SRQR) or double- (DRQR) residue of the quadratic response function of the electric dipole operator[53] within the framework of TDDFT.[54] TPA cross section calculations with DRQR are carried out using the sum-over-state (SOS) method. These calculations were carried out the the Dalton program.

larger than the corresponding MAE obtained with the PBE0 and B3LYP functionals. As illustrated for C152, the large deviations between B3LYP and CAMB3LYP can be attributed to the value of β (see Table 1S in the Supporting Information Section), since $\beta = 0$ for B3LYP ($\alpha = 0.19$ nearly the same as in B3LYP). Thus, the α and β parameters must be reexamined for both the ground (e.g. the G2 set) and excited states. However, the effects of β on the ground state energetics are found to be small. The MAE of atomization in the G2 set for $\beta = 0$ and $\beta = 0.46$ changes from 2.68 kcal/mol to 2.53 kcal/mol, respectively.[40] Thus, the corresponding error for $\beta = \alpha = 0.19$ (Eq. 2) is likely within this range. The small compromise in the ground state energetics results in a significant improvement in the predicted S_0-S_1 ICT energies, which have MAEs of 0.10 and 0.06 eV (without C153 due to convergence problem) for the 6-311G(d,p) and 6-311++G(d,p) basis sets, respectively. It is worth noting that excitation energies computed with the nonhybrid BLYP functional and Tamm-Dancoff approximation are computationally more economical but do not offer comparable accuracy delivered by TDDFT with the hybrid B3LYP, PBE0, or *m*CAMB3LYP functional. The predicted[30,31] gas-phase S_0-S_1 energies of 2.99 and 2.90 eV for C152A (C35) and C153, respectively, are significantly lower than the corresponding experimental values[6] of 3.56 and 3.37 eV. For C151, the BLYP and SAOP gas phase excitation energies of 3.32[30,31] and 3.24 eV,[32] respectively, were reported. These predicted values are much lower than the experimental value of 3.70 eV in *n*-hexane.[12]

We now discuss the trends observed with the predicted results in the gas-phase, which do not appear to be dependent upon the choice of basis and functionals. For example, the B3LYP and PBE0 (0.17 eV) S_0-S_1 shifts for C152-C153 are identical for the 6-311G** and 6-311++G** basis sets. The predicted value of 0.17 eV is in good agreement with the corresponding experimental value of 0.22 eV. All four functionals predict the S_0-S_1 energy to shift to the red with increasing degree of alkylation, C120 <C1 <C480. A trifluorine substitution at the 4-methyl group gives pronounced red shifts that increase in magnitude with higher degree of alkylation (C151 < C307 <C152 <152A < C522 <C153), in agreement with the experiment data[6] for the latter four coumarins. We should note that the absorption maxima of C152 and C152A listed in Table 1 of Ref. [6] must be interchanged for them to be consistent with their corresponding absorption spectra given in Figure 3.

The continuum solvation models do not treat specific solvent-solute interactions such H-bonding, which is important in water[8,24] and methanol[55] but not in a cyclohexane solution. For the 6-311G(d,p)

basis set, the SCRF-S model of cyclohexane overestimates the experimental S_0-S_1 energies by 0.05, 0.22, and 0.42 eV for the B3LYP, *m*CAMB3LYP, and CAMBLYP, respectively. Using the same basis set, the errors (MAE) for PCM with PBE0 and B3LYP are 0.03 and 0.11 eV, respectively. These excitation energies do not appear to be strongly affected by the addition of diffuse functions, which are found to lower the energies by 0.05-0.07 eV for C120 (see Table 1). Thus, the 6-311G(d,p) basis set seems adequate for predicting S_0-S_1 energies. Note that the errors for B3LYP are slightly improved compared to those obtained in the gas-phase due to the effects of compensation in excitation energy by the SCRF-S method and the B3LYP functional. This might be attributed to the tendency to overestimate and underestimate the excitation energy by the SCRF-S model and the B3LYP functional, respectively. Consequently, the *m*CAMB3LYP and CAMBLYP energies that are overestimated in the gas-phase, are exacerbated in the SCRF-S model. For B3LYP, the SCRF-S excitation energies are larger (by 0.03-0.07 eV) compared to the corresponding PCM (with MAE of 0.03 eV) values. This suggests that excitation energies of *m*CAMB3LYP and CAMBLYP are likely improved with the PCM model and the use of diffuse functions, assuming the reduction in excitation energy observed in C120 holds for other coumarins. Thus, using PCM with more flexible basis sets might bring the *m*CAMB3LYP errors closer to those obtained with PBE0 (MAE of 0.11 eV). However, it is unlikely that using PCM with larger basis sets would bring the CAMB3LYP errors to an acceptable range for these systems. Overall, we found the predicted B3LYP and PBE0 S_0-S_1 energies in cyclohexane are in excellent agreement with experiment. The error for *m*CAMB3LYP and CAMB3LYP are slightly larger than those obtained in the gas-phase. The trends predicted for the gas-phase S_0-S_1 energy to shift to the red with increasing degree of alkylation for the nonfluorinated (C120 <C1 <C480) and for the trifluorinated series (C151 < C307 <C152 <152A < C522 <C153) also hold true in cyclohexane, and are confirmed by a collection of experimental values in different studies.

For ethanol, the SCRF-S and the PCM models appear to overestimate S_0-S_1 energies, suggesting the H-bonding effects are significant, especially in C120 and C151. The overall errors for PCM, however,

remain low for B3LYP (0.11 eV) and PBE0 (0.21 eV). The MAEs using the SCRF-S model are 0.13, 0.27, and 0.48 eV for the B3LYP, *m*CAMB3LYP, and CAMBLYP, respectively. The latter two functionals overestimate all the S_0-S_1 excitation energies, with C120 having the largest error. In fact, the continuum solvation models fail to predict the observed blueshift in the excitation energy in water with respect to EtOH (see Table 1). This might be attributed to the H-bonding, which is not accounted for in the continuum models of solvation. In C120 (and C151), water and alcoholic solvents can form hydrogen bonds with the nitrogen (A) or oxygen (B) at the amine and the carbonyl groups, respectively, and/or accepting an H-bond at the amine hydrogens (C).[55-57] The B and C interactions strongly stabilize the positive and negative charges on the amino nitrogen and carbonyl oxygen, respectively, in ICT excited state of C120, leading to a red shift in the ICT excitation energy in the more acidic water compared to alcohols. The A and B interactions are present in all 7-aminocoumarins while the C interactions are unique to the non-alkylated and the N-alkylated (not N-dialkylated) systems. However, the blueshift in the S_0-S_1 excitation energy in water with respect to alcohols has been attributed to the A interaction that better stabilizes the ground state than the ICT excited state.[56,57] Interestingly, previous DFT studies of C151 with one water molecule did not locate a stable A-type conformer in the ground state. Therefore, calculations of C120 in water and methanol clusters embedded in a dielectric continuum are important to shed more light on the effects on H-bonding on the solution spectra. Thus, we have carried out PCM-TDDFT calculations on C120 with small number of water and methanol molecules. Although some conformers with the A and C interactions possess blueshifts in excitation energies, the computed Boltzmann averaged excitation energies (neglecting entropy) are similar for water and methanol. The inclusions of entropy, which requires more sophisticated treatments for low frequencies modes beyond the so called rigid rotor and harmonic oscillator approximation, are under consideration. Calculations for larger clusters using Monte Carlo optimization[58] are also being carried out and will be reported in the future.

We now consider the OPA intensity, which can be measured with the μ_{ge} or f values that are available for C152[59] and C153[11] in a number of solvents. For C153, the emission and absorption transition moments were reported to be the same to within the experimental uncertainty.[11] For other systems, the μ_{ge} and f values in solutions were obtained by using published maxima of absorption coefficients and corresponding full-width at half maxima (FWHM), and by integrating the appropriate spectral bands, which were approximated by Gaussians. Although gas-phase absorption spectra for a number of coumarins have been reported, the corresponding absolute intensities were not measured, except for the f value of 0.37 for C153,[7] which is within the range (0.33-0.44) of the computed values. For other systems, our comparison between theory and experiment is largely limited to values obtained in alcoholic solutions. Experimental f values in cyclohexane and water are also reported for some systems.

The value of f for C120 in water (0.325) was obtained by digitization of the OPA spectrum reported by Overway et al.[18] The corresponding value in ethanol (0.318) was obtained from the spectral data reported by Fisher et al.[16] and Reynolds and Drexhage.[60] These experimental oscillator strengths are slightly smaller than the computed values of about 0.4-0.5, with those predicted by CAMB3LYP and *m*CAMB3LYP functionals being the larger ones (see Table 1). The transition dipoles and oscillator strengths obtained with the PCM model are also slightly larger than the corresponding SCRF-S values. The overall errors for PCM, however, remain low for B3LYP (0.41 D) and PBE0 (0.55 D). The MAEs using the SCRF-S model are 0.28, 0.48, and 0.71 D for the B3LYP, *m*CAMB3LYP, and CAMBLYP, respectively. It is encouraging that the predicted *m*CAMB3LYP transition dipoles are in accordance with those of B3LYP and PBE0. The predicted changes in μ_{ge} from cyclohexane to MeOH/EtOH are small. This is consistent with the lack of dependence on solvents for absorption transition moments of C102 and C153, as observed by Lewis and Maroncelli.[11]

Upon alkylation, the computed μ_{ge} and f values of the ICT band show a slight increase, as predicted by the PCM model using the PBE0 (0.07, 0.61 D) and B3LYP (0.07, 0.64 D) functionals for C1. This is in good agreement with the experimental shift of 0.08 and 0.74 D for the oscillator strength and transition moment, respectively. Note that these observed shifts are also well reproduced using the SCRF-S model with the B3LYP (0.08, 0.68 D) and the *m*CAMB3LYP (0.10, 0.74 D) functionals but not as accurate with the CAMB3LYP (0.12, 0.79 D) functional. The alkylation of C120 to create C480 produces a similar increase (0.09, 0.95 D) in the experimental f and μ_{ge} values from the absorption data of Fisher et al.[16,19] and of Reynolds and Drexhage.[60] However, the corresponding computed values for the *syn* and *anti* conformations of C480 show smaller increases from that of C120, which is overestimated by the continuum solvation models. Furthermore, the two isoenergetic *syn* conformations are 0.5 and 0.2 kcal/mol lower in energy than their *anti* counterparts in the gas-phase and in MeOH, respectively. Thus, rapid *syn-anti* conversions may occur at room temperature, leading to a different mixture of conformers and corresponding intensities for the ICT band. Similarly, the *syn* conformers of the trifluorine substituted C153 are 0.3 kcal/mol lower in energy than their *anti* counterparts in the gas-phase. This is identical to the *syn-anti* relative energy reported by Cave et al.[29] However, recent calculations by Sulpizi et al.[30,31] for C153 using the nonhybrid BLYP functional with a plane-wave basis set and pseudopotentials revealed that the *anti* conformer has the lowest energy. The other *anti* conformer was located at 0.8 kcal/mol above the lowest *anti* congener. The two *syn* conformers were found to be 0.8 and 1.1 kcal/mol above the lowest *anti* structure. We found that the *syn* and *anti* conformers of C153 are isoenergetic in EtOH.

The shifts in transition moment for the trifluorine derivatives follow the alkylation trends discussed above, increasing from C151 (4.97 D) < C307 (5.52 D), C152 (5.31 D) < C152A (5.88 D), C153 (5.71 D). The predicted transition moments (5.23-5.69 D) for C151 are significantly larger than experimental value (4.97 D) in EtOH due to the importance of H-bonding. For C153, the predicted transition values vary from 5.84 D (B3LYP) to 6.40 D (CAMB3LYP). The corresponding experimental value of 5.71 D

was obtained by using the peak extinction coefficient reported by Reynolds and Drexhage[60] and the FWHM reported by Gustavsson et al.[12] This value is in good agreement with the transition dipole moments of 5.03-5.71 D reported by Lewis and Maroncelli[11] for C153 in methanol, as obtained by numerically integrating the spectrum and scaling them with different refractive index correction factors. Their non-scaled value of 5.80 D for the emissive transition dipole moment, which was reported to be the same as the absorptive moment, is slightly (0.1 D) larger than the value integrated with Gaussian lineshape above. The predicted errors of 0.3-0.4 D for B3LYP and *m*CAMB3LYP are close to the estimated experimental uncertainty of 0.3 D (5%) for C153.[11]

B. Two-Photon Absorption

The TPA absorption cross sections are listed in Tables 2, 3, and 4 for various basis sets and functionals along with available cross sections. In addition, cross sections obtained with experimental μ_{ge} (in Table 1) and the difference between the ground and first excited state ($\Delta\mu_{ge}$) dipole moments using the two-state approximation are also listed for four coumarins. These experimental $\Delta\mu_{ge}$ have been estimated by several experimental methods, including time-resolved microwave dielectric absorption measurements,[61] which is claimed to be superior. Note that these experimental studies were not carried in the same solvents as in the TPA studies. Thus, the cross sections obtained from these quantities offer qualitative rather than quantitative comparisons with the TPA measurements. The consensus in OPA intensity lineshape at room (or higher) temperature appears to be Gaussian. However, both Gaussian and Lorentzian functions are often used to compute TPA cross sections. The difference between two line shape functions, as illustrated for C120 in Table 2, is a factor of 1.48, with the Gaussian cross (δ_G) section being larger than the corresponding Lorentzian (δ_L) value. TPA cross sections computed with the single residue of the quadratic response function are denoted by SRQR. DRQR-SOS refers to values computed with the SOS method using the DFT ground state dipoles, transition dipoles and excitation energies from linear response TDDFT, excited dipoles and excited-to-excited transition dipoles from the double residue quadratic response function. The latter approach is

computationally more demanding, but offers insights into the mechanism of TPA. For C120 with the lowest five excited states in the SOS expression, the two methods yield cross sections at the TPA resonance within a few GM of each other (see Table 2). Our SOS calculations reveal a type II TPA for the first state of C120, in which the TPA is driven by $\Delta\mu_{ge}$. Thus, the difference in the cross sections obtained from the two-state and the five-state approximation is (1-3 GM) small (cf. Tables 2 and 3). We found that the cross sections are not significantly affected by the basis set. For C120, changes of δ_G upon going from the 6-31G(d) to the 6-311++G(d,p) basis set using the SRQR method are less than one GM for all functionals. For the largest basis set, variations in the peak cross sections are within 2 GM, as obtained with CAMB3LYP (5.5 GM), PBE0 (6.9 GM) , and B3LYP (7.1 GM) functionals. Small variations among the functionals are also observed in solvents for C120 and other systems.

In solvents, the predicted cross sections of 13-14 GM for C120 (Table 4) are significantly larger than those in the gas-phase, due to the increase in $\Delta\mu_{ge}$ (Table 3). The cross sections predicted by PCM are significantly larger than those obtained with the SCRF-S using the two-state approximation. This can be attributed to larger excited state dipole moments predicted by PCM. It is not straightforward to compare these computed values with experiment, since the TPA cross sections of 19 and 14 GM measured at 3.29 and 4.13 eV in ethanol[16] and water,[18] respectively, are not the local maxima of the TPA spectra. The maxima are likely located at higher (lower) energy with even larger cross sections than the predicted values for ethanol (water). Interestingly, these cross sections fall in the range (2-26 GM) of values obtained for the two-state approximation using experimental μ_{ge} and $\Delta\mu_{ge}$.

The predicted TPA cross section (energy) increases (decreases) with increasing degree of alkylation. This is consistent with the increase in $\Delta\mu_{ge}$ and μ_{ge} upon alkylation that has been predicted[29] and experimentally observed.[61] However, the increase in the cross-section upon increasing degree of alkylation (C120 <C1 <C480) is not quantitatively reproduced. The experimental cross sections of 104 and 160 GM for C1 and C480 (Table 4) are significantly larger than the corresponding predicted values of 28 (C1) and 22 (C480) GM. These discrepancies can be attributed to the uncertainty both in the

predicted and observed cross sections. In addition to the errors from the line width functions as discussed above, the computed errors might be attributed to the specific solvent interactions that are not accounted for in the SCRF model. Experimentally, the errors for TPA cross sections for C1 and C120 have been reported of about half order of magnitude.[16] For C480 (C102), the TPA cross section was obtained by relative fluorescence measurement[19] assuming unity fluorescence quantum yield for both the *p*-bis-*o*-methyl-styrylbenzene (BMSB) reference and C480, which was reported to be 0.58[60] to 0.95[9] in EtOH. Very high (0.995-0.870) quantum yields were reported for BMSB in a few nonpolar solvents, but was not given for EtOH.[62] Thus, an adjustment the TPA cross section of C480 based on measured quantum yields would be useful.

For the trifluorinated series, the predicted TPA cross sections follow the alkylation trends previously observed. The TPA maximum (δ_G) cross section (energy) is predicted (SCRF-S-B3LYP/6-311G**) to increase (decrease) from 14.0 GM (3.45 eV) to 25.1 GM (3.17 eV) for C151 and C307, respectively. The TPA spectrum of C151 in EtOH taken from 2.95 eV to 3.28 eV show a cross section of 47 GM at 3.28 eV,[16] which is comparable to the OPA maximum of 3.24 eV in the same solvent. The experimental TPA cross section of 47 GM for C151 is more than twice maximum cross section of $19\eta \pm$ 5.5 GM obtained in MeOH at 3.20 eV for C307,[17] even with the fluorescence quantum yield $\eta = 1$. Thus, the observed redshift in the TPA maximum of C151 upon alkylation is consistent with the theoretical prediction. However, the decrease in the corresponding cross section is in discordance with theory. It should be noted that the experimental cross section of 47 GM reported for C151 has a much larger uncertainty (half order of magnitude)[16] than that of C307. Thus, new experimental studies on the TPA cross sections of C151 and other coumarins would useful in verifying the predicted results.

4. Summary and Conclusions

We found that gas-phase excitation energies for C152, C152A, C522, and C153 are well reproduced with the 6-311G(d,p) basis set, with the mean absolute errors of 0.03, 0.08, 0.10, and 0.32 eV, for PBE0, B3LYP, *m*CAMB3LYP ($\alpha = 0.19$ and $\beta = 0.19$), and CAMB3LYP ($\alpha = 0.19$ and $\beta = 0.46$) respectively.

The corresponding set of 0.16, 0.05, 0.06, and 0.29 eV are found for the 6-311++G(d,p), which has negligible differences in S_0-S_1 excitation energies and oscillator strengths from the larger aug-cc-pVTZ basis set. All the four functionals predict S_0-S_1 energy to shift to the red with increasing degree of alkylation. Trifluorination at the 4-methyl group gives pronounced red shifts that increase in magnitude with higher degree of alkylation. These predictions are found to be in agreement with experiment.

The 6-311G(d,p) excitation energies predicted by the SCRF-S model overestimate experimental S_0-S_1 energies by 0.05, 0.22, and 0.42 eV for the B3LYP, *m*CAMB3LYP, and CAMBLYP, respectively, in cyclochexane. In MeOH/EtOH, the MAEs for excitation energy (transition moment) are 0.13 (0.28), 0.27 (0.48), and 0.48 (0.71) eV (D) for the B3LYP, *m*CAMB3LYP, and CAMBLYP, respectively. The corresponding MAEs for the PCM model are 0.11 (0.41) and 0.21(0.55) eV (D) for B3LYP and PBE0, respectively. The larger errors of excitation energy predicted in alcoholic solvents are attributed to the H-bonding, which is not accounted for in the continuum solvation models.

The first excited state of coumarins have large TPA cross sections, which are driven by the change in dipole moments between the ground and the more polar first excited state. We observed large enhancement in the TPA cross section in polar solvents due to the increase in excited state dipole moments compared to the corresponding ground state values. We found that the variations in the TPA peak cross sections are small (1-3 GM) among the various basis sets and functionals, including the *m*CAMB3LYP functional which significantly reduces the errors in the TPA and OPA resonances. The predicted cross sections are largely consistent with experiment to within the experimental uncertainties. Some large deviations may be attributed to the large uncertainties in the experimental cross sections. Thus, new experimental TPA studies for these coumarins would be useful in verifying the predicted results.

Table 1. 6-311G(d,p) Excitation energy (E, eV), oscillator strength (*f*), and transition dipole moment (μ_{01}, D) for coumarin derivatives compared with experiment. Values in parentheses and brackets are computed with the 6-311++G(d,p) and the aug-cc-pVTZ basis sets.

		Theory		Expt	
System/Method	$E(S_1)$	*f*	μ_{01}	Energy (μ_{01}) [*f*]	Solvent
C120					
CAMB3LYP	4.29 (4.24)	0.373 (0.368)	4.79 (4.79)		
PBE0	4.09 (4.04) [4.03]	0.348 (0.363) [0.355]	4.74 (4.87)[4.82]		
B3LYP	4.00 (3.94) [3.93]	0.329 (0.344)[0.338]	4.66 (4.80) [4.76]		
					EtOH
[o]SCRF-S-CAMB3LYP	4.07 (4.00)	0.479 (0.497)	5.57 (5.72)		
[o]SCRF-S-*m*CAMB3LYP	3.90 (3.83)	0.433 (0.451)	5.41 (5.57)		
PCM-PBE0	3.81 (3.74)	0.456 (0.477)	5.61 (5.80)		
[o]SCRF-S-B3LYP	3.76 (3.69)	0.390 (0.406)	5.23 (5.39)		
PCM-B3LYP	3.71 (3.64)	0.424 (0.445)	5.49 (5.68)	3.51[a](5.54) [0.318][c,h]	
					Water
[p]SCRF-S-CAMB3LYP	(3.99)	(0.495)	(5.72)		
[p]SCRF-S-*m*CAMB3LYP	(3.81)	(0.447)	(5.56)		
[p]SCRF-S-B3LYP	(3.68)	(0.401)	(5.36)		
PCM-B3LYP	3.70 (3.63)	0.418 (0.439)	5.46 (5.65)	3.65 (4.85) [0.325][b]	
					Cyclohexane

Table 1. Cont.

qSCRF-S-CAMB3LYP	4.19 (4.13)	0.467 (0.477)	5.42 (5.51)		
qSCRF-S-*m*CAMB3LYP	4.02 (3.97)	0.434 (0.446)	5.33 (5.44)		
qSCRF-S-B3LYP	3.89 (3.84)	0.401 (0.415)	5.22 (5.33)		
PCM-PBE0	3.93 (3.87)	0.472 (0.495)	5.63 (5.81)		
PCM-B3LYP	3.84 (3.77)	0.443 (0.468)	5.52 (5.72)	3.76[a]	
C1					
CAMB3LYP	4.09	0.495	5.65		
*m*CAMB3LYP	3.89	0.449	5.52		
PBE0	3.82	0.433	5.46		
B3LYP	3.72 (3.66) [3.65]	0.401 (0.409) [0.405]	5.33 (5.43) [5.41]		
					EtOH
qSCRF-S-B3LYP	3.55	0.452	5.79		
qSCRF-S-CAMB3LYP	3.90	0.598	6.36		
qSCRF-S-*m*CAMB3LYP	3.69	0.529	6.15		
PCM-PBE0	3.57	0.529	6.25		
PCM-B3LYP	3.47	0.490	6.10	3.32[a] (5.63) [0.399][h,i]	
					Cyclohexane
rSCRF-S-CAMB3LYP	3.99	0.606	6.33		
rSCRF-S-*m*CAMB3LYP	3.79	0.546	6.17		

Table 1. Cont.

[r]SCRF-S-B3LYP	3.62	0.488	5.96		
PCM-PBE0	3.67	0.548	6.27		
PCM-B3LYP	3.57	0.510	6.13	3.54[b]	
C480					
CAMB3LYP (*syn*)	3.97	0.432	5.35		
*m*CAMB3LYP (*syn*)	3.76	0.391	5.23		
B3LYP (*syn*)	3.60	0.347	5.04		
					MeOH
[o]SCRF-S-CAMB3LYP (*syn*)	3.78	0.524	6.05		
[o]SCRF-S-*m*CAMB3LYP (*syn*)	3.57	0.462	5.84		
[o]SCRF-S-B3LYP (*syn*)	3.41	0.406	5.60		
PCM-B3LYP (*anti*)	3.33	0.447	5.95		
PCM-PBE0 (*syn*)	3.44	0.467	5.98		
PCM-B3LYP (*syn*)	3.34	0.433	5.85	3.19 (5.84) [0.412][h,n]	
					Cyclohexane
[r]SCRF-S-CAMB3LYP	3.88	0.529	6.00		
[r]SCRF-S-*m*CAMB3LYP	3.67	0.475	5.84		
[r]SCRF-S-B3LYP	3.51	0.422	5.63		
PCM-PBE0	3.55	0.488	6.02		

Table 1. Cont.

PCM-B3LYP	3.45	0.455	5.89	3.43[d]	
C151					
CAMB3LYP	4.07	0.382	4.97		
*m*CAMB3LYP	3.88	0.347	4.85		
B3LYP	3.73 (3.66) [3.67]	0.312 (0.320) [0.317]	4.70 (4.80) [4.77]		
TDA-BLYP[s]	3.32				
SAOP/TZP[t]	3.24				
					EtOH
[o]SCRF-S-CAMB3LYP	3.78	0.464	5.69		
[o]SCRF-S-*m*CAMB3LYP	3.59	0.406	5.46		
[o]SCRF-S-B3LYP	3.44 (3.41)	0.356 (0.382)	5.68 (5.44)		
PCM-PBE0	3.48	0.425	5.68		
PCM-B3LYP	3.38	0.393	5.54	3.24 (4.97) [0.304][c]	
					n-hexane
MD-QMMM-SAOP/TZP[t]	3.07			3.70[j]	
					Cyclohexane
[r]SCRF-S-CAMB3LYP	3.94	0.457	5.53		
[r]SCRF-S-*m*CAMB3LYP	3.75	0.410	5.37		
[r]SCRF-S-B3LYP	3.60	0.366	5.18		

Table 1. Cont.

PCM-PBE0	3.63	0.412	5.66		
PCM-B3LYP	3.53	0.411	5.54	3.56[e]	
C307					
CAMB3LYP	3.90	0.429	5.38		
*m*CAMB3LYP	3.70	0.389	5.27		
PBE0	3.64	0.376	5.22		
B3LYP	3.55	0.352	5.12		
					MeOH
[o]SCRF-S-CAMB3LYP	3.54	0.521	6.23		
[o]SCRF-S-*m*CAMB3LYP	3.33	0.453	5.99		
[o]SCRF-S-B3LYP	3.16	0.398	5.77		
PCM-PBE0	3.36	0.461	6.02		
PCM-B3LYP	3.27	0.431	5.89	3.15 (5.52) [0.364][f]	
					Cyclohexane
[r]SCRF-S-CAMB3LYP	3.77	0.530	6.09		
[r]SCRF-S-*m*CAMB3LYP	3.57	0.479	5.94		
[r]SCRF-S-B3LYP	3.42	0.433	5.78		
PCM-PBE0	3.47	0.480	6.04		
PCM-B3LYP	3.38	0.451	5.93	3.37[d]	

Table 1. Cont.

C152					
CAMB3LYP	3.88 (3.86)	0.468 (0.477)	5.64 (5.71)		
*m*CAMB3LYP	3.66 (3.62)	0.408 (0.405)	5.42 (5.43)		
PBE0	3.58 (3.51)	0.383 (0.379)	5.31 (5.34)		
B3LYP	3.48 (3.40)	0.352 (0.348)	5.17 (5.20)	3.59[g]	
					EtOH
ꟾSCRF-S-CAMB3LYP	3.46	0.542	6.43		
ꟾSCRF-S-*m*CAMB3LYP	3.22	0.453	6.09		
ꟾSCRF-S-B3LYP	3.03	0.387	5.80		
PCM-PBE0	3.30	0.462	6.08		
PCM-B3LYP	3.20	0.427	5.93	3.13[b](5.31) [0.334][m]	
C152A (C35)					
CAMB3LYP	3.84 (3.83)	0.496 (0.497)	5.83 (5.85)		
*m*CAMB3LYP	3.62 (3.59)	0.432 (0.424)	5.61 (5.58)		
PBE0	3.54 (3.47)	0.407 (0.404)	5.51 (5.54)		
B3LYP	3.44 (3.35)	0.375 (0.372)	5.37 (5.41)	3.56[g]	
TDA-BLYP[s]	2.99				
					EtOH
ꟾSCRF-S-CAMB3LYP	3.51	0.593	6.68		

Table 1. Cont.

[q]SCRF-S-*m*CAMB3LYP	3.28	0.504	6.37		
[q]SCRF-S-B3LYP	3.09	0.437	6.10		
PCM-PBE0	3.26	0.493	6.32		
PCM-B3LYP	3.16	0.457	6.18	3.10[d](5.88) [0.408][h,j]	
					Cyclohexane
[r]SCRF-S-CAMB3LYP	3.70	0.614	6.61		
[r]SCRF-S-*m*CAMB3LYP	3.48	0.535	6.37		
[r]SCRF-S-B3LYP	3.30	0.468	6.11		
PCM-PBE0	3.37	0.510	6.32		
PCM-B3LYP	3.27	0.473	6.17	3.30[d]	
C522					
CAMB3LYP	3.80 (3.79)	0.466 (0.493)	5.68 (5.86)		
*m*CAMB3LYP	3.59 (3.57)	0.415 (0.436)	5.52 (5.67)		
PBE0	3.51 (3.44)	0.397 (0.396)	5.46 (5.51)		
B3LYP	3.42 (3.34)	0.370 (0.368)	5.34 (5.39)	3.45[g]	
					EtOH
[a]SCRF-S-CAMB3LYP	3.49	0.568	6.56		
[a]SCRF-S-*m*CAMB3LYP	3.28	0.496	6.31		
[a]SCRF-S-B3LYP	3.12	0.437	6.08		

Table 1. Cont.

PCM-PBE0	3.23	0.497	6.37		
PCM-B3LYP	3.14	0.463	6.24	3.05[d]	
					Cyclohexane
[b]SCRF-S-CAMB3LYP	3.66	0.572	6.42		
[b]SCRF-S-*m*CAMB3LYP	3.45	0.508	6.23		
[b]SCRF-S-B3LYP	3.28	0.452	6.03		
PCM-PBE0	3.34	0.508	6.34		
PCM-B3LYP	3.24	0.475	6.21	3.25[d]	
C153					
CAMB3LYP	3.72	0.444	5.61		
*m*CAMB3LYP	3.49	0.385	5.41		
TDA-BLYP[s]	2.90				
PBE0	3.41 (3.34)	0.359 (0.360)	5.27 (5.33)		
B3LYP	3.31 (3.23)	0.331 (0.333)	5.14 (5.21)	3.37[g] (5.51)[0.37][k]	
					EtOH
[a]SCRF-S-CAMB3LYP	3.44	0.534	6.40		
[a]SCRF-S-*m*CAMB3LYP	3.23	0.456	6.11		
[a]SCRF-S-B3LYP	3.06	0.396	5.84		
PCM-PBE0	3.13	0.454	6.19		

Table 1. Cont.

PCM-B3LYP	3.04	0.422	6.05	2.95[d](5.71) [0.373][j]
				Cyclohexane
[b]SCRF-S-CAMB3LYP	3.59	0.541	6.30	
[b]SCRF-S-*m*CAMB3LYP	3.37	0.469	6.06	
[b]SCRF-S-B3LYP	3.20	0.407	5.79	
PCM-PBE0	3.24	0.468	6.18	
PCM-B3LYP	3.15	0.434	6.03	3.15[d](5.84) [0.408][l]

[a]Ref. [14]. [b]Ref. [18]. [c]Ref. [16]. [d]Ref. [9]. [e]Ref. [63]. [f]Rogers, J. E. private communication. [g]Experimental gas-phase S_0-S_1, Ref. [6]. [h]Ref. [60]. [i]Ref. [64]. [j]Ref. [12]. [k]Ref. [7]. [l]Ref. [11]. [m]Ref. [59]. [n]Ref. [19].

[o]a_0 = 10.00 au, ε = 24.55, n^2 = 1.847. [p]a_0 = 10.0 au, ε = 78.39, n^2 = 1.776

[q]a_0 = 11.00 au, ε = 24.55, n^2 = 1.847. [r]a_0 = 11.0 au, ε = 2.023, n^2 = 2.028

[s]Ref. [31]. [t]Ref. [32], excitation energy in *n*-hexane was obtained from an average of 400 snapshot of the MD simulations.

Table 2. S_1 TPA cross section (in GM, using FWHM = 0.2 eV) and excited state maximum (in parentheses) for C120[a]

	SRQR		DRQR-SOS (5)	
Method	δ_G	δ_L	δ_G	δ_L
CAMB3LYP/6-31G*	5.1 (4.34)	3.6 (4.34)	6.8 (4.35)	4.7 (4.35)
PBE0/6-31G*	6.4 (4.13)	4.4 (4.13)	6.9 (4.14)	4.7 (4.14)
B3LYP/6-31G*	6.6 (4.03)	4.6 (4.04)	6.9 (4.05)	4.8 (4.05)
CAMB3LYP/6-311G**	5.2 (4.30)	3.7 (4.30)	6.5 (4.31)	4.4 (4.31)
PBE0/6-311G**	6.5 (4.10)	4.5 (4.10)	6.5 (4.12)	4.5 (4.11)
B3LYP/6-311G**	6.7 (4.01)	4.7 (4.01)	6.8 (4.02)	4.7 (4.01)
CAMB3LYP/6-311++G**	5.5 (4.25)	3.9 (4.25)	5.9 (4.26)	4.0 (4.26)
PBE0/6-311++G**	6.9 (4.06)	4.8 (4.06)	6.8 (4.07)	4.7 (4.07)
B3LYP/6-311++G**	7.1 (3.96)	5.0 (3.96)	7.0 (3.97)	4.9 (3.97)
[b]SCRF-S-B3LYP/6-311++G**	13.9 (3.69)	9.5 (3.69)	17.4 (3.70)	11.7 (3.69)
[b]SCRF-S-CAMB3LYP/6-311++G**	13.2 (4.00)	9.0 (4.00)	15.5 (4.01)	10.6 (4.01)
[c]SCRF-S-B3LYP/6-311++G**	14.1 (3.70)	9.6 (3.70)	17.6 (3.72)	11.9 (3.71)
[c]SCRF-S-CAMB3LYP/6-311++G**	13.8 (4.01)	8.9 (4.01)	15.3 (4.03)	10.5 (4.02)

[a]Experimental TPA cross section of 19 GM (not a maximum value) measured at 3.29 eV in ethanol,[16]; experimental TPA cross section of 14 GM (not a maximum value) measured at 4.13 eV in water.[18]

[b]a_0 = 10.00 au, ε = 78.39, n^2 = 1.776 (water)

[c]a_0 = 10 au, ε = 24.55, n^2 = 1.847 (EtOH)

Table 3. Ground and excited state dipole moments (in D) and TPA cross sections for C120 using the two-state approximation.

Method	μ_0	μ_{S1}	μ_{S2}	μ_{S3}	δ_G	Solvent.
CAMB3LYP/6-31G*	6.3	8.3	7.5	2.6	4.8	
PBE0/6-31G*	6.4	9.0	8.3	2.4	7.5	
B3LYP/6-31G*	6.3	9.1	8.4	2.2	8.2	
CAMB3LYP/6-311G**	6.4	8.3	7.4	2.6	5.0	
PBE0/6-311G**	6.4	8.9	8.1	2.3	7.6	
B3LYP/6-311G**	6.4	9.1	8.2	2.2	8.3	
CAMB3LYP/6-311++G**	6.7	8.5	7.4	2.6	4.7	
PBE0/6-311++G**	6.6	9.0	8.3	2.2	7.3	
B3LYP/6-311++G**	6.7	9.2	8.3	2.1	8.0	
Experiment[a]		7.9				
						EtOH
PCM-PBE0/6-31G*	9.4	14.5	12.3	3.7	33.6	
PCM-B3LYP/6-31G*	9.4	14.5	12.4	3.7	33.0	
PCM-PBE0/6-311G**	9.6	14.7	12.0	11.7	34.9	
PCM-B3LYP/6-311G**	9.6	14.8	12.2	11.4	34.4	
[d]SCRF-S-CAMB3LYP/6-311++G**	9.5	12.6	10.5	11.4	14.5	
[b]SCRF-S-B3LYP/6-311++G**	9.6	13.4	11.2	10.5	19.1	
						Water
PCM-B3LYP/6-311G**	9.8	15.2	12.4	11.7	36.5	
[d]SCRF-S-CAMB3LYP/6-311++G**	9.7	12.8	10.7	11.7	14.6	
PCM-B3LYP/6-311++G**	10.4	15.9	13.0	12.3	42.0	
[d]SCRF-S-B3LYP/6-311++G**	9.8	13.6	11.4	10.8	18.9	

[a]Estimated from the Lippert-Mataga relationship using μ_g value of 6.0 D and r value of 3.41 Å.[14]

[b]a_0 = 10.00 au, ε = 24.55, n^2 = 1.847 (EtOH). [d]a_0 = 10.00 au, ε = 78.39, n^2 = 1.776 (water)

Table 4. Computed TPA cross section (in GM, using FWHM = 0.2 eV) and excited state maximum (in parentheses) compared with experiment

	SQR		Expt.	
System/Method	δ_G	δ_L	δ	δ_G (TS)[e]
C120				
B3LYP/6-311++G**	7.1 (3.96)	5.0 (3.96)		
[a]SCRF-S-*m*CAMB3LYP/6-311++G**	13.7 (3.82)	9.3 (3.82)		
[a]SCRF-S-CAMB3LYP/6-311++G**	13.2 (4.00)	9.0 (4.00)		
[a]SCRF-S-B3LYP/6-311++G**	14.1 (3.70)	9.6 (3.70)	14 (4.13)[f*]	4[e,j]
[b]SCRF-S-CAMB3LYP/6-311++G**	13.8 (4.01)	8.9 (4.01)		
[b]SCRF-S-*m*CAMB3LYP/6-311++G**	13.8 (3.84)	9.4 (3.84)		
[b]SCRF-S-B3LYP/6-311++G**	13.9 (3.69)	9.5 (3.69)	19 (3.29)[g*]	
C1				
B3LYP/6-311G**	18.6 (3.73)	12.7 (3.73)		
[c]SCRF-S-CAMB3LYP/6-311G**	26.2 (3.91)	17.8 (3.91)		
[c]SCRF-S-*m*CAMB3LYP/6-311G**	28.0 (3.70)	19.2 (3.70)		
[c]SCRF-S-B3LYP/6-311G**	28.6 (3.53)	19.6 (3.53)	104 (3.29)[g*]	8[e,k]
C480 (C102)				
B3LYP/6-311G** (*syn*)	14.9 (3.61)	10.2 (3.61)		
[d]SCRF-S-CAMB3LYP/6-311G** (*syn*)	21.7 (3.79)	14.9 (3.79)		
[d]SCRF-S-*m*CAMB3LYP/6-311G** (*syn*)	22.1 (3.58)	15.2 (3.58)		
[d]SCRF-S-B3LYP/6-311G** (*syn*)	21.7 (3.42)	14.8 (3.42)	160 (3.17)[i]	9[e,l]
C151				
B3LYP/6-311G**	10.3 (3.74)	7.1 (3.74)		
[c]SCRF-S-B3LYP/6-311G**	14.0 (3.45)	9.5 (3.45)	47 (3.28)[g*]	14[e,m]
[c]SCRF-S-*m*CAMB3LYP/6-311G**	15.4 (3.60)	10.5 (3.60)		
[c]SCRF-S-CAMB3LYP/6-311G**	16.8 (3.79)	11.5 (3.79)		
C307				

B3LYP/6-311G**	15.4 (3.56)	10.5 (3.56)	
[d]SCRF-S-CAMB3LYP/6-311G**	29.0 (3.55)	19.8 (3.55)	
[d]SCRF-S-*m*CAMB3LYP/6-311G**	27.1 (3.34)	18.5 (3.34)	
[d]SCRF-S-B3LYP/6-311G**	25.1 (3.17)	17.1 (3.17)	19η (3.20)[h]

[a]a_0 = 10 au, ε = 78.39, n^2 = 1.776 (water)

[b]a_0 = 10 au, ε = 24.55, n^2 = 1.847 (EtOH)

[c]a_0 = 11 au, ε = 24.55, n^2 = 1.847 (EtOH)

[d]a_0 = 11 au, ε = 32.63, n^2 = 1.758 (MeOH)

[e]TPA cross sections are obtained with experimental μ_{ge} in Table 1, $\Delta\mu_{ge}$ from time-resolved microwave dielectric absorption measurements in benzene,[61] computed angles (C120 = 160°, C1 = 165 °, C480 = 164°, C151 = 164°) between μ_{ge} and $\Delta\mu_{ge}$, and Gaussian lineshapes (FWHM = 0.2 eV) using the two-state approximation.

[f]Experimental TPA cross section measured in water.[18]

[g]Experimental TPA cross section measured in EtOH (relative error of about 1/2 of magnitude).[16]

[h]Experimental TPA maximum cross section measured in MeOH, η is the quantum yield.[17] η = 0.61,[57] 0.56[60] in EtOH. η = 0.90 in 50% EtOH.[9]

[i]Experimental TPA maximum cross section measured in MeOH.[19]

[j]$\Delta\mu_{ge}$ = 2.4 D, using $\Delta\mu_{ge}$ = 4.1-6.2 D (electrooptic)[61] gives δ_G (TS) = 11-26 GM using $\Delta\mu_{ge}$ = 1.90 D[14] (solvatochromism) gives δ_G (TS) = 2 GM. using $\Delta\mu_{ge}$ = 3.97 D[65] (solvatochromism) gives δ_G (TS) = 11 GM.

[k]$\Delta\mu_{ge}$ = 2.9 D, using $\Delta\mu_{ge}$ = 7.3-7.8 D[61] (electrooptic) gives δ_G (TS) = 50-57 GM, using $\Delta\mu_{ge}$ = 2.72 D[15] (solvatochromism) gives δ_G (TS) = 7 GM.

[l]$\Delta\mu_{ge}$ = 3.0 D, using $\Delta\mu_{ge}$ = 2.11 D[66] (solvatochromism) gives δ_G (TS) = 4 GM

[m]$\Delta\mu_{ge}$ = 4.4 D, using $\Delta\mu_{ge}$ = 1.7 D[66] (solvatochromism) gives δ_G (TS) = 2 GM, using $\Delta\mu_{ge}$ = 2.81 D[63] (solvatochromism) gives δ_G (TS) = 6 GM, using $\Delta\mu_{ge}$ = 4.35-7.01 D[5] (electrooptic) gives δ_G (TS) = 14-35 GM,

*Not a maximum value

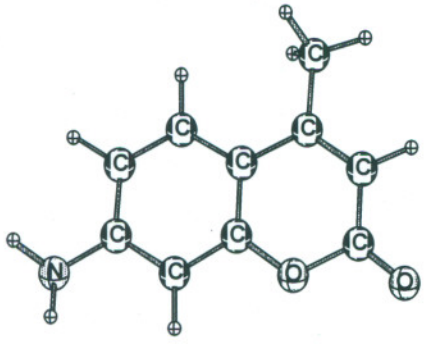

C120

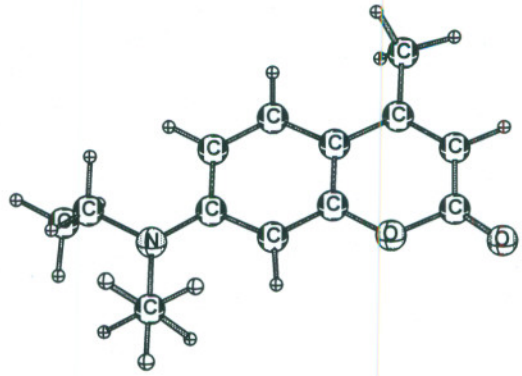

C1 (C481)

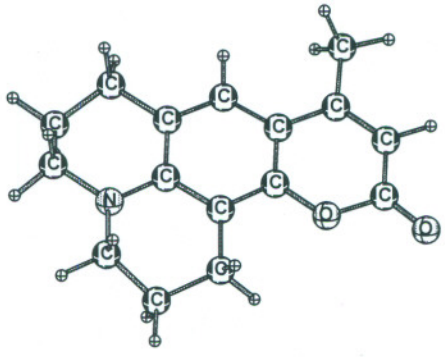

C480 (*syn*)

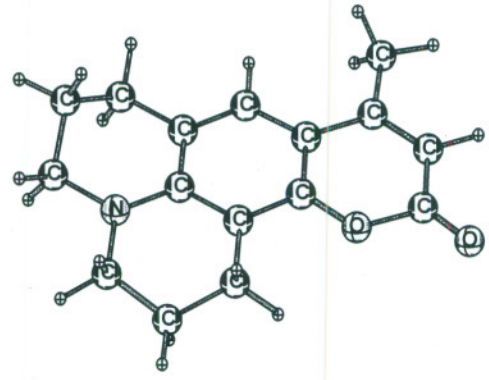

C480 (*anti*)

Figure 1. Structure of coumarin 120, 1, 480 (102).

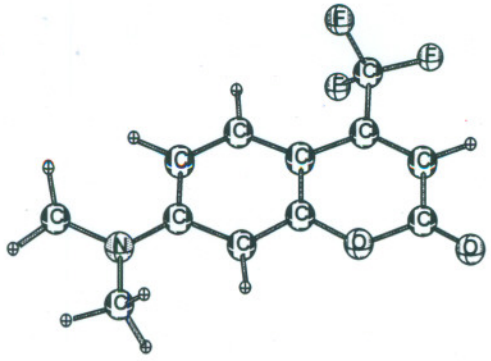

C152

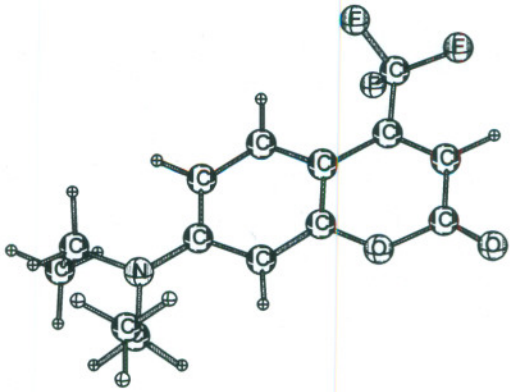

C152A (C35)

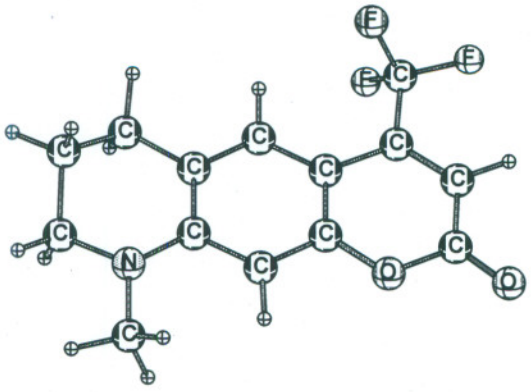

C522

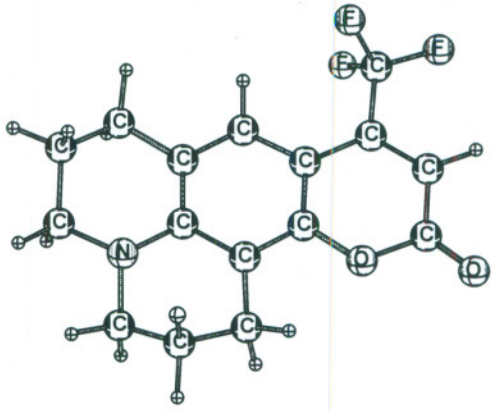

C153

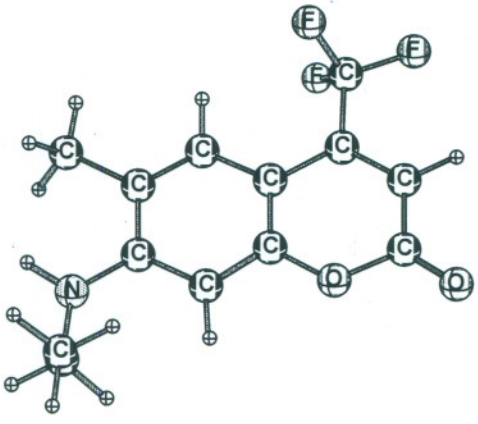

C307

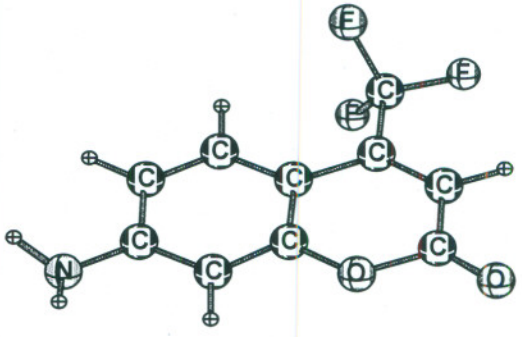

C151

Figure 2. Structure of coumarin 152, 152A, 522, 153, 307, and 151.

Acknowledgements

This research has been supported by the Air Force Office of Scientific Research (AFOSR) and by CPU time from the Aeronautical Systems Center (ASC) Major Shared Resource Center (MSRC). We gratefully acknowledge a copy of the Dalton program with the CAMB3LYP functional from Prof. Hans Agren and useful discussions with Dr. Joy Rogers, AFRL/MLPJ.

Reference:

(1) Pavlopoulos, T. G. *IEEE J. Quantum Electronics* **1972**, *9*, 510.
(2) Pavlopoulos, T. G.; Hammond, P. R. *J. Am. Chem. Soc.* **1974**, *96*, 6568.
(3) Moerner, W. E.; Silence, S. M. *Chem. Rev.* **1994**, *94*, 127.
(4) Moylan, C. R. *J. Phys. Chem.* **1994**, *98*, 13513.
(5) Memkovich, N. A.; Reis, H.; Baumann, W. *J. Lumin.* **1997**, *71*, 255.
(6) Ernsting, N. P.; Asimov, M.; Schafer, F. P. *Chem. Phys. Lett.* **1982**, *91*, 231.
(7) Muhlpfordt, A.; Schanz, R.; Ernsting, N. P.; Farztdinov, V.; Grimme, S. *Phys. Chem. Chem. Phys.* **1999**, *1*, 3209.
(8) Pryor, B. A.; Palmer, P. M.; Andrews, P. M.; Berger, M. B.; Topp, M. R. *J. Phys. Chem. A* **1998**, *102*, 3284.
(9) Jones II, G.; Jackson, W. R.; Choi, C.-Y.; Bergmark, W. R. *J. Phys. Chem.* **1985**, *89*, 294.
(10) Fee, R. L.; Milsom, J. A.; Maroncelli, M. *J. Phys. Chem.* **1991**, *95*, 5170.
(11) Lewis, J. E.; Maroncelli, M. *Chem. Phys Lett.* **1998**, *282*, 197.
(12) Gustavsson, T.; Cassara, L.; Gulbinas, V.; Gurzadyan, G.; Mialocq, J. C.; Pommeret, S.; Sorgius, M.; van der Meulen, P. *J. Phys. Chem. A* **1998**, *102*, 4229.
(13) Chowdhury, A.; Locknar, S. A.; Premvardhan, L. L.; Peteanu, L. A. *J. Phys. Chem. A* **1999**, *103*, 9614.
(14) Pal, H.; Nad, S.; Kumbhakar, M. *J. Chem. Phys.* **2003**, *119*, 443.
(15) Barik, A.; Nath, S.; Pal, H. *J. Chem. Phys.* **2003**, *119*, 10202.
(16) Fisher, A.; Cremer, C.; Stelzer, E. H. K. *Appl. Opt.* **1995**, *34*, 1989.
(17) Xu, C.; Webb, W. W. *J. Opt. Soc. Am. B* **1996**, *13*, 481.
(18) Overway, K. S.; Lytle, F. E. *Appl. Spectrosc.* **1998**, *52*, 298.
(19) Fisher, W. G.; Wachter, E. A.; Lytle, F. E.; Armas, M.; Seaton, C. *App. Spectrosc.* **1998**, *52*, 536.
(20) McCarthy, P. K.; Blanchard, G. J. *J. Phys. Chem.* **1993**, *97*, 12205.
(21) Novak, I.; Kovac, B. *J. of Elect. Spectrosc. and Related Phenomena* **2000**, *113*, 9.
(22) Kovac, B.; Novak, I. *Spectrochim. Acta, A* **2002**, *58*, 1483.
(23) Martins, L. R.; Skaf, M. S. *Chem. Phys Lett.* **2003**, *370*, 683.
(24) Cave, R. J.; Burke, K.; Castner Jr., E. W. *J. Phys. Chem. A* **2002**, *106*, 9294.
(25) Runge, E.; Gross, E. K. U. *Phys. Rev. Lett.* **1984**, *52*, 997.
(26) Bauernschmitt, R.; Ahlrichs, R. *Chem. Phys. Lett.* **1996**, *256*, 454.
(27) Casida, M.; Jamorski, C.; Casida, K. C.; Salahub, D. R. *J. Chem. Phys.* **1998**, *108*, 4439.
(28) Stratmann, R. E.; Scuseria, G. E.; Frisch, M. J. *J. Chem. Phys.* **1998**, *109*, 8218.
(29) Cave, R. J.; Castner Jr., E. W. *J. Phys. Chem. A* **2002**, *106*, 12117.
(30) Sulpizi, M.; Carloni, P.; Hutter, J.; Rothlisberger, U. *Phys. Chem. Chem. Phys.* **2003**, *5*, 4798.
(31) Sulpizi, M.; Rohrig, U. F.; Hutter, J.; Rothlisberger, U. *Int. J. Quantum Chem.* **2005**, *101*, 671.
(32) Neugebauer, J.; Jacob, C. R.; Wesolowski, T. A.; Baerends, E. J. *J. Phys. Chem. A* **2005**, *109*, 7805.
(33) Ingrosso, F.; Ladanyi, B. M.; Menucci, B.; Scalmani, G. *J. Phys. Chem. B* **2006**, *110*, 4953.
(34) Becke, A. D. *J. Chem. Phys* **1993**, *98*, 5648.
(35) Becke, A. D. *Phys. Rev. A* **1988**, *38*, 3098.
(36) Lee, C.; Yang, W.; Parr, R. G. *Phys. Rev. B* **1988**, *37*, 785.
(37) Day, P. N.; Nguyen, K. A.; Pachter, R. *J. Phys. Chem. B* **2005**, *109*, 1803.

(38) Ernzerhof, M.; Scuseria, G. E. *J. Chem. Phys.* **1999**, *110*, 5029.
(39) Adamo, C.; Scuseria, G. E.; Barone, V. *J. Chem. Phys.* **1999**, *111*, 2889.
(40) Yanai, T.; Tew, D. P.; Handy, N. C. *Chem. Phys. Lett.* **2004**, *393*, 51.
(41) Peach, M. J. G.; Helgaker, T.; Salek, P.; Keal, T. W.; Lutnaes, O. B.; Tozer, D. J.; Handy, N. C. *Phys. Chem. Chem. Phys* **2006**, *8*, 558.
(42) Kohn, W.; Sham, L. J. *Phys. Rev. A* **1965**, *140*, 1133.
(43) Krishnan, R.; Binkley, J. S.; Seeger, R.; Pople, J. A. *J. Chem. Phys.* **1980**, *72*, 650.
(44) Frisch, M. J.; Trucks, G. W.; Schlegel, H. B.; Scuseria, G. E.; Robb, M. A.; Cheeseman, J. R.; Montgomery, J. A., Jr.; Vreven, T.; Kudin, K. N.; Burant, J. C.; Millam, J. M.; Iyengar, S. S.; Tomasi, J.; Barone, V.; Mennucci, B.; Cossi, M.; Scalmani, G.; Rega, N.; Petersson, G. A.; Nakatsuji, H.; Hada, M.; Ehara, M.; Toyota, K.; Fukuda, R.; Hasegawa, J.; Ishida, M.; Nakajima, T.; Honda, Y.; Kitao, O.; Nakai, H.; Klene, M.; Li, X.; Knox, J. E.; Hratchian, H. P.; Cross, J. B.; Adamo, C.; Jaramillo, J.; Gomperts, R.; Stratmann, R. E.; Yazyev, O.; Austin, A. J.; Cammi, R.; Pomelli, C.; Ochterski, J. W.; Ayala, P. Y.; Morokuma, K.; Voth, G. A.; Salvador, P.; Dannenberg, J. J.; Zakrzewski, V. G.; Dapprich, S.; Daniels, A. D.; Strain, M. C.; Farkas, O.; Malick, D. K.; Rabuck, A. D.; Raghavachari, K.; Foresman, J. B.; Ortiz, J. V.; Cui, Q.; Baboul, A. G.; Clifford, S.; Cioslowski, J.; Stefanov, B. B.; Liu, G.; Liashenko, A.; Piskorz, P.; Komaromi, I.; Martin, R. L.; Fox, D. J.; Keith, T.; Al-Laham, M. A.; Peng, C. Y.; Nanayakkara, A.; Challacombe, M.; Gill, P. M. W.; Johnson, B.; Chen, W.; Wong, M. W.; Gonzalez, C.; Pople, J. A. Gaussian 03; A.11.4 ed.; Gaussian, Inc.: Pittsburgh PA, 2003.
(45) Dalton. a molecular electronic structure program, Release 2.0, http://www.kjemi.uio.no/software/dalton/dalton.html, 2005.
(46) Cossi, M.; Scalmani, G.; Rega, N.; Barone, V. *J. Chem. Phys.* **2002**, *117*, 43.
(47) Cossi, M.; Barone, V. *J. Chem. Phys.* **2001**, *115*, 4708.
(48) Mikkelsen, K. V.; Dalgaard, E.; Swanstrom, P. *J. Chem. Phys.* **1987**, *91*, 3081.
(49) Sutherland, R. L. *Handbook of Nonlinear Optics*; Marcel Dekker, Inc.: New York, 1996.
(50) Goppert-Mayer, M. *Ann. Physik.* **1931**, *9*, 273.
(51) Masthay, M. B.; Findsen, L. A.; Pierce, B. M.; Bocian, D. F.; Lindsey, J. S.; Birge, R. R. *J. Chem. Phys.* **1986**, *84*, 3901.
(52) Peticolas, W. L. *Ann. Rev. Phys. Chem.* **1967**, *18*, 233.
(53) Olsen, J.; Jørgensen, P. *J. Chem. Phys.* **1985**, *82*, 3235.
(54) Salek, P.; Vahtras, O.; Guo, J.; Luo, Y.; Helgaker, T.; Agren, H. *Chem. Phys. Lett.* **2003**, *374*, 446.
(55) Palmer, P. M.; Chen, Y.; Topp, M. R. *Chem. Phys Lett.* **2000**, *321*, 62.
(56) Arbeloa, T. L.; Arbeloa, F. L.; Tapia, M. J.; Arbeloa, I. L. *J. Phys. Chem.* **1993**, *97*, 4704.
(57) Arbeloa, T. L.; Arbeloa, F. L.; Arbeloa, I. L. *J. Lumi.* **1996**, *68*, 149.
(58) Day, P. N.; Pachter, R.; Gordon, M. S.; Merrill, G. N. *J. Chem. Phys.* **2000**, *112*, 2063.
(59) Vijila, C.; Ramalingam, A. *J. Mater. Chem.* **2001**, *11*, 749.
(60) Reynolds, G. A.; Drexhage, K. H. *Opt Commun.* **1975**, *13*, 222.
(61) Samanta, A.; Fessenden, R. *J. Phys. Chem. A* **2000**, *104*, 8577.
(62) Bush, T. E.; Scott, G. W. *J. Phys. Chem.* **1981**, *85*, 144.
(63) Nad, S.; Pal, H. *J. Phys. Chem. A* **2001**, *105*, 1097.
(64) Du, H.; Fuh, R. A.; Corkan, J. L.; Lindsey, J. S. *Photochem. Photobio.* **1998**, *68*, 141.
(65) Ghazy, R.; Azim, S. A.; Shaheen, M.; El-Mekawey, F. *Spectrochim. Acta A* **2004**, *60*, 187.
(66) Ravi, M.; Soujanya, T.; Samanta, A.; Radhakrishnan, T. P. *J. Chem. Soc. Faraday Trans.* **1995**, *91*, 2739.